IEEE Access
Multidisciplinary | Rapid Review | Open Access Journal

SPECIAL SECTION ON KEY ENABLING TECHNOLOGIES FOR PROSUMER ENERGY MANAGEMENT

Received November 12, 2020, accepted November 27, 2020, date of publication December 2, 2020, date of current version December 14, 2020.

Digital Object Identifier 10.1109/ACCESS.2020.3041709

Real-Time Optimal Operation Control of Micro Energy Grid Coupling With Electricity-Thermal-Gas Considering Prosumer Characteristics

SU AN[1,2], (Graduate Student Member, IEEE), HONGLEI WANG[1,3], AND XUFENG YUAN[4]

[1]Management Department, Guizhou University, Guiyang 550025, China
[2]Power Dispatching Control Center, Guizhou Power Grid Company Ltd., Guiyang 550001, China
[3]Key Laboratory of "Internet+" Collaborative Intelligent Manufacturing, Guizhou University, Guiyang 550025, China
[4]Electrical Engineering Department, Guizhou University, Guiyang 550025, China

Corresponding author: Honglei Wang (gzdxhlwang@163.com)

This work was supported by the National Natural Science Foundation of China under Grant 71962004, in part by the Key Laboratory of "Internet+" Collaborative Intelligent Manufacturing in Guizhou Province under Grant [2016]5103 and in part by the National Natural Science Foundation of China under Grant 52067004.

ABSTRACT Under the increasingly stringent environmental regulations, the installed capacity of distributed renewable energy is increasing rapidly. How to fully absorb renewable energy without affecting power grid security and ensuring power quality is the key problem to be solved. The rapid development of energy production, conversion and storage equipment of prosumer makes the operation of micro energy grid possible. Therefore, according to the energy characteristics of different prosumer, this article divides the micro energy grid into two types: micro energy grid of electricity selling and micro energy grid of energy supplying. The constrained nonlinear optimization method is used to solve the optimization problem of this high-dimensional nonlinear system with time delay. In this article, the comparative study of optimal operation control between the two kinds of micro energy grid is carried out. In order to deal with the uncertainty of distributed renewable energy output and load forecasting deviation, this article proposes a real time adaptive dynamic optimization control strategy based on deep learning. The strategy uses deep learning technology to pretrain the action network, so as to learn the optimal operation behavior of micro energy grid. Finally, the online simulation of micro energy grid for consecutive days is used to verify the correctness and real-time performance of the algorithm.

INDEX TERMS Micro energy grid, distributed renewable energy, adaptive dynamic optimization, deep learning.

I. INTRODUCTION

The energy revolution characterized by the deep integration of new energy and information technology is promoting the development of traditional energy system to smart energy system. As the most critical technologies supporting the development of smart energy system, artificial intelligence, big data, blockchain and Internet of things (IOT) have been widely concerned [1], [2]. How to construct an efficient intelligent energy system to support the coordinated optimization and complementarity of multiple energy sources, improve the energy efficiency management level of smart grid and energy Internet, and strengthen the application of distributed multi energy agents in micro grid and regional integrated energy system is the focus of current research [3], [4].

Long-distance transmission of large-scale intermittent renewable energy will bring a lot of charging reactive power, resulting in the rise of falling point voltage. The power grid also needs to invest a lot of reactive power compensation equipment which have high cost of investment and operation [5]. In addition, the power grid also needs to provide plenty of spinning reserve [6], which greatly increases the difficulty of power grid operation, and reduces the dynamic stability of power grid. In this case, if we want to make full

The associate editor coordinating the review of this manuscript and approving it for publication was Bin Zhou.

use of renewable energy, it is necessary to develop various energy forms coordinated and complementary. That is, the joint optimization operation of Micro Energy Grid (MEG) with electric power, gas and heat energy. In addition, for the remote underdeveloped areas with wind, solar, water and gas resources, such as Africa, Tibet and Guizhou of western China, we can build MEG system according to local conditions, rely on the clean energy complementary system to solve the energy demand problem in remote areas, and establish a commercialized energy supply market. However, the coordination and complementarity of multiple energy sources increases the complexity of MEG combined systems. Because of the different models and characteristics of different energy forms, the traditional reduction method of analyzing each energy network separately has been difficult to adapt the coupled integrated energy system [7]–[9].

In recent years, the construction speed of wind and photovoltaic plants is extremely fast, and the installed capacity far exceeds the capacity in use. If only relying on the traditional power grid to balance, it is difficult to avoid large scale wind and solar power curtailment. Therefore, it is necessary to study the integration optimal operation of energy storage equipment and microgrid, such as electric vehicle charging and exchange station, combined cooling, heating and power (CCHP) and so on, and propose the method and algorism of optimization operation of MEG [10]–[12]. For the intelligent energy system with coupled multi-energy, only electrical energy can completely replace other energy sources. For example, the heat demand of users can be provided by air conditioning or gas boilers. However, the motor of manufacturing control, television and other equipment of users can only use electric energy, which cannot be replaced by other energy sources. Therefore, it is of great practical significance to study the power grid as the main energy system of multi-energy. At the same time, most of the distributed renewable energy in mountain area and virtual power plants on the user side are connected to the power grid through the voltage level of 10kV and below, so the research on the optimal operation of the integrated energy system should focus on the distribution network and micro grid level.

There have been some studies on optimal operation of micro energy grid. In terms of the type of operation equipment, the research has gradually changed from a traditional Micro Grid (MG) with distributed energy to a multi-energy microgrid with energy storage equipment, Power to Gas (P2G) and virtual power plant [13]–[18]. Aiming at the traditional MG with Distributed Generation (DG), an analytical target cascading method is proposed to implement autonomous optimized economic dispatch [13]. On the basis of traditional MG, the operation of Battery Energy Storage System (BESS) is included in the optimization in [14], and a consensus algorithm based distributed optimization method is proposed. In order to improve the complementary ability of MGs, fuel cell, micro turbine and boiler are included in the unified optimization of MG in [15], and a cooperative game approach is developed to study the benefit distribution among MG. Considering the limit in the energy form independence and operation mode, a dispatching model based on electric thermal gas coupling microgrid is proposed [16], and the operation of MG is optimized. Based on the Integrated Energy System (IES), the Integrated Electrical Natural Gas System with Microgrid (IENGS-M) is established in [17], and the multi-objective optimization of the system is carried out with the minimum cost and pollution as the objective. In [18], the Integrated Energy Campus Microgrid (IECM) is optimized, and the time delay of energy transmission in cooling / heating and gas pipelines is studied particularly. From the perspective of optimization method and algorism, most of the related research uses distributed optimization methods to solve the optimization problem among MG. Bi-level optimizations are used to coordinate different optimization objectives, and robust optimization and multi-scenario method are used to deal with the uncertainty of renewable energy output [19]–[25]. An effective distributed stochastic optimal scheduling scheme with minimum information exchange is proposed to dynamically optimize energy conversion and storage devices in the multi-energy system [19]. Two distributed dynamic optimization strategies to respectively study the Economic Dispatch Problem (EDP) under both cases without and with generation constraints are proposed in [20],[21]. In [22], a fully distributed method by using the exact diffusion strategy which can achieve exact convergence under sparse communication network is developed, and the simulation is carried out in multiple scenarios. Reference [23] propose a bi-level optimal low-carbon economic dispatch model to solve the integrated energy supply of an industrial park and optimize the energy conversion efficiency. Bi-level adjustable robust optimization model is studied and compared to different strategies for the operation of a multi-energy system considered as a systemic optimization problem in [24],[25]. Due to the uncertainty of renewable energy and the large number of multi-energy equipment with different operation time scale, the optimization of MEG is usually to solve a high-dimensional, nonlinear and complex problem. Therefore, the research on MEG optimization mainly focuses on the time scale of day-ahead or within-day [26]–[30], and there is relatively less research on real-time online optimization. In order to improve the calculation speed, the second-order cone relaxation of the branch flow equations method is use to solve the problem [26]. In order to solve the day-ahead scheduling problem of integrated energy network with identifying redundant gas network constraints, [27] develops a bound tightening strategy combines Weymouth equation relaxation and an optimality-based bounds tightening method. Mixed-Integer Second-Order Cone Programming (MISOCP) method is used by [28] to achieve microgrid day-ahead operation. In [29] and [30], the operation of MG is optimized by using the hierarchical genetic algorithm and multi objective evolution algorithm respectively.

Nowadays, the idea and method of machine learning is developing rapidly, and it is gradually used to solve the problems in power system. With the development of computing

ability and algorithm, reinforcement learning and deep learning technology have been used to solve renewable energy output forecasting, user side load forecasting and complex system optimization [31]–[35]. In [31] and [32], deep neural network and meta-model techniques are used to learn the behavior of MG and determine the optimal operating schedules of the heat generation equipment. Furthermore, a multi-agent deep reinforcement learning approach is used to optimize the post-disaster control of islanded MG [33]. To execute real-time control of MG, a deep convolution neural network and cooperative game approach is proposed in [34]. In [35], reinforcement learning is used to optimized energy management strategy for a hybrid electric vehicle.

According to the above research, the study on multi-energy system including distributed renewable energy, electric or thermal energy storage device and electric vehicle is relatively scattered, there is little research on how to match different types of MEG with corresponding equipment and user types, and makes analysis and comparison between them. At the same time, for MEG operation optimization problems, robust optimization is mostly used to solve the uncertainty of variables. However, with the increase of variable dimension and the nonlinearity of constraints in time-delay systems, the optimization algorithm is difficult to meet the needs of real time.

Based on the above challenges and motivations, the main contributions of this article can be listed as follows:

1) According to the character of users in MEG and the operation objectives of MEG operators, the integrated energy systems with multi energy and equipment are classified into two types of MEG, and their operation models are designed.

2) For these two kinds of MEG, the nonlinear optimization method is used to achieve the optimal solution, and the comparative study of optimal operation between the two kinds of micro energy grid is carried out. The optimization results of continuous days are used to train the deep neural network to learn the optimal operation behavior of MEGs.

3) Combining the deep training neural network with adaptive dynamic programming technology, this article proposes a real time adaptive dynamic optimization algorithm based on deep learning to solve the uncertainty of renewable energy sources and users' demand in MEG. Then, the algorism is verified by online simulation of MEG for consecutive days.

II. MICRO ENERGY GRID SYSTEM

According to the energy characteristics of prosumer and the role played by MEG in the distribution network, the MEG is divided into two types: Micro Energy Grid of Electricity Selling (MEG-E) and Micro Energy Grid of Energy Supply (MEG-S).

For the MEG-E, the main goal of this type of prosumer is to fully absorb renewable energy. While ensuring the energy demand of users in the grid, they should sell power to the distribution network as much as possible during the period of high electricity price to obtain profits. This kind of MEG mainly includes photovoltaic, wind power, electric vehicle

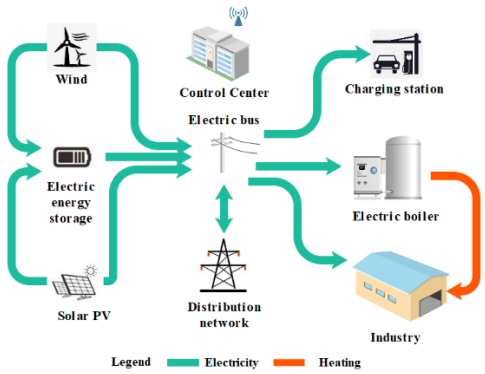

FIGURE 1. The structure of the MEG-E system.

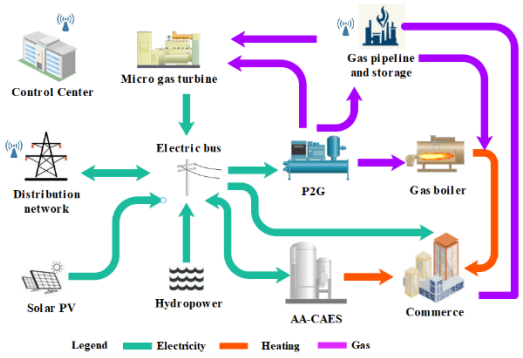

FIGURE 2. The structure of the MEG-S system.

charging station and electric energy storage equipment. At the same time, the operator of MEG-E makes the most profit by choosing to cooperate with industrial users for matching with the generation characteristics of renewable energy, which is shown in Fig. 1. For the MEG-S, the main goal of its operator is to meet the demand of users for various types of energy, and obtain profits by selling electricity, natural gas and heat energy to users. This kind of MEG-S mainly includes photovoltaic, micro gas turbine, gas boiler, P2G equipment, small hydropower units and other equipment. In order to obtain the maximum profit from energy sales, the operator tends to networking with commercial users, which is shown in Fig. 2. This article mainly studies on the existing grid structure (the power or natural gas networks necessary for the operation of P2G and other devices have been built). Therefore, building a new power or natural gas network or change the distribution network structure to achieve better operation effect is not in the scope of the study.

III. PROBLEM FORMULATION

A. MATHEMATICAL MODEL OF MEG-E

1) OBJECTIVE FUNCTION

The operation cost of MEG-E mainly includes the cost of purchasing electricity from distribution network (C_{elec}^{MEG-E}), the cost of purchasing ancillary services from the distribution network (C_{anc}^{MEG-E}), Operating cost of energy

storage device (C_{bess}^{MEG-E}). The revenue includes the revenue from selling clean electricity to the distribution network (I_{grid}^{MEG-E}), revenue from electricity sales to Electric Vehicle Charging Stations (EVCS) (I_{evcs}^{MEG-E}), revenue from electricity and heat sales to industrial users ($I_{user-elec}^{MEG-E}$, $I_{user-heat}^{MEG-E}$.) Therefore, the objective function is described by (1).

$$\begin{aligned} min\ & C_{MEG-E} \\ &= C_{elec}^{MEG-E} + C_{anc}^{MEG-E} + C_{bess}^{MEG-E} \\ &\quad - I_{grid}^{MEG-E} - I_{evcs}^{MEG-E} - I_{user-elec}^{MEG-E} - I_{user-heat}^{MEG-E} \end{aligned} \tag{1}$$

$$C_{elec}^{MEG-E} = \sum_{t=1}^{T} u_{buy}^{MEG\text{-}E}(t) \times \tau_{buy}^{grid}(t) \times P_{elec}^{MEG-E} \tag{2}$$

$$C_{anc}^{MEG-E} = C_{anc-ss}^{MEG-E} + C_{anc-spin}^{MEG-E} \tag{3}$$

$$C_{anc-ss}^{MEG-E} = R_m \times (\tau_{ss}^{anc-gas} N_{gas-ss}^{grid} + \tau_{ss}^{anc-hydro} N_{hydro-ss}^{grid}) \tag{4}$$

$$C_{anc-spin}^{MEG-E} = R_m \times \left[\begin{array}{l} \tau_{spin}^{anc-gas} \sum_{t=1}^{T} \sum_{j=1}^{J} \left(u_{spin}^{anc\text{-}gas}(t) \left(P_{j,gas}^{grid}(t) - \alpha_{spin} S_{j,gas}^{grid} \right) \right) \\ + \tau_{spin}^{anc-hydro} \sum_{t=1}^{T} \sum_{k=1}^{K} \\ \quad \left(u_{spin}^{anc-hydro}(t) \left(P_{k,gas}^{grid}(t) - \alpha_{spin} S_{k,hydro}^{grid} \right) \right) \end{array} \right] \tag{5}$$

$$R_m = \frac{\sum_{t=1}^{T} u_{sell}^{m}(t) P_{elec}^{m}(t)}{\sum_{n=1}^{M} \sum_{t=1}^{T} u_{sell}^{m}(t) P_{elec}^{m}(t)} \tag{6}$$

$$C_{bess}^{MEG\text{-}E} = \alpha_s \times P_{bess}^{MEG-E}(t)^2 + \beta_s \tag{7}$$

$$I_{grid}^{MEG-E} = \sum_{t=1}^{T} u_{sell}^{MEG-E}(t) \times \tau_{elec}^{MEG-E}(t) \times P_{elec}^{MEG-E}(t) \tag{8}$$

$$I_{eves}^{MEG-E} = \sum_{t=1}^{T} \tau_{eves}^{MEG-E}(t) \times P_{eves}^{MEG-E}(t) \tag{9}$$

$$I_{user\text{-}elec}^{MEG-E} = \sum_{t=1}^{T} \tau_{user\text{-}elec}^{MEG-E}(t) \times P_{user\text{-}elec}^{MEG-E}(t) \tag{10}$$

$$I_{user\text{-}leat}^{MEG-E} = \sum_{t=1}^{T} \tau_{user\text{-}heat}^{MEG-E}(t) \times Q_{user\text{-}heat}^{MEG-E}(t) \tag{11}$$

MEG-E is connected to Distribution Network (DN) through distribution transformer. When the Distributed Renewable Energy (DRE) output in MEG-E is relatively low, the cost of power purchasing from DN can be expressed in (2). $P_{elec}^{MEG-E}(t)$ is the transformer exchange power at time t. $u_{buy}^{MEG-E}(t)$ is the 0-1 variable ($u_{buy}^{MEG-E}(t) = 1$,when $P_{elec}^{MEG-E}(t) > 0$). $\tau_{elec}^{grid}(t)$ is the price of purchasing electricity from DN.

The distribution network provides auxiliary services for the connected MEG-E. In order to fully absorb renewable energy, the distribution network operator need to dispatch the gas power units and hydropower units to start or stop and keep a certain proportion of rotating reserve to balance the fluctuation of distributed renewable energy generation. The total cost of auxiliary services is shared by MEG-Es connected to DN, and can be represented as (3)-(6). C_{anc-ss}^{MEG-E} and $C_{anc-spin}^{MEG-E}$ are start-stop cost and spinning reserve cost. R_m is the cost sharing coefficient of ancillary services. $u_{sell}^{m}(t)$ is the 0-1 variable ($u_{sell}^{m}(t) = 1$,when $P_{elec}^{MEG-E}(t) < 0$). N_{gas-ss}^{grid} and $N_{hydro-ss}^{grid}$ are start-stop times of gas turbine and hydropower unit in DN. $\tau_{ss}^{anc-gas}$ and $\tau_{ss}^{anc-hydro}$ are the cost of each start-stop of these two units. $P_{j,gas}^{grid}(t)$ and $P_{k,hydro}^{grid}(t)$ are output of the gas turbine j and the hydropower unit k at time t. S_{gas}^{grid} and S_{hydro}^{grid} are the rated capacity of gas turbine and hydropower unit. α_{spin} is the spinning reserve factor. $u_{j,spin}^{grid-gas}(t)$ and $u_{k,spin}^{grid-hydro}(t)$ are 0-1 variables indicating whether there is a spinning reserve at time t. $\tau_{spin}^{anc-gas}$ and $\tau_{spin}^{anc-hydro}$ are unit price of spinning reserve for gas and hydropower units.

The BESS in MEG-E plays a role in smoothing the output curve of distributed generation. It can also improve the power supply quality of user side and provide power support for the system when the output of distributed generation decreases greatly in a short time. However, the service life of BESS decreases with the increase of charging and discharging times, and its operation cost can be represented as (7). $P_{bess}^{MEG-E}(t)$ is output of battery energy storage system at time t. a_s is penalty factor of fast charging and discharging and β_s is operating cost factor of BESS.

Besides, $P_{evcs}^{MEG-E}(t)$ is charging power of EVCS at time t. $\tau_{evcs}^{MEG-E}(t)$ is the price of electricity selling by MEG-E to EVCS at time t. $P_{user-elec}^{MEG-E}(t)$ and $Q_{user-heat}^{MEG-E}(t)$ are electricity load and heat load of industrial users at time t. $\tau_{user-elec}^{MEG-E}(t)$ and $\tau_{user-heat}^{MEG-E}(t)$ are price of electricity and heat at time t.

2) MODEL CONSTRAINTS

The constraints of MEG-E can be given as below:

$$\begin{aligned} &P_{elec}^{MEG-E}(t) + P_{bess}^{MEG-E}(t) + P_{evcs}^{MEG-E}(t) + P_{user\text{-}elec}^{MEG-E}(t) \\ &+ P_{elec\text{-}boiler}^{MEG-E}(t) - P_{wind}^{MEG-E}(t) - P_{pv}^{MEG-E}(t) = 0 \end{aligned} \tag{12}$$

$$Q_{user\text{-}heat}^{MEG\text{-}E}(t) = u_{elec\text{-}boiler} \times P_{elec\text{-}boiler}^{MEG-E}(t) \tag{13}$$

$$-S_{elec}^{trans} \le P_{elec}^{MEG\text{-}E}(t) \le S_{elec}^{trans} \tag{14}$$

$$u_{buy}^{MEG\text{-}E}(t) + u_{sell}^{MEG-E}(t) = 1 \tag{15}$$

$$-P^{max}_{bess,\,disc} \le P^{MEG-E}_{bess}(t) \le P^{max}_{bess\,,c} \quad (16)$$

$$E^{MEG-E}_{bess}(t+1) = E^{MEG-E}_{bess}(t) + P^{MEG-E}_{bess}(t) \quad (17)$$

$$SOC_{min} \le SOC(t) \le SOC_{max} \quad (18)$$

$$0 \le P^{MEG-E}_{wind}(t) \le S^{max}_{wind} \quad (19)$$

$$-P^{max}_{wind} \le P^{MEG-E}_{wind}(t+1) - P^{MEG-E}_{wind}(t) \le P^{max}_{wind} \quad (20)$$

$$0 \le P^{MEG-E}_{pv}(t) \le S^{max}_{pv} \quad (21)$$

$$-P^{max}_{pv} \le P^{MEG-E}_{pv}(t+1) - P^{MEG-E}_{pv}(t) \le P^{max}_{pv} \quad (22)$$

$$0 \le P^{MEG-E}_{elec-boiler}(t) \le S^{max}_{elec-boiler} \quad (23)$$

$$-P^{max}_{elec-boiler} \le P^{MEG-E}_{elec-boiler}(t+1) - P^{MEG-E}_{elec-boiler}(t) \le P^{max}_{elec-boiler} \quad (24)$$

$$P^{min}_{evcs} \le P^{MEG-E}_{evcs}(t) \le P^{max}_{evcs} \quad (25)$$

$$\sum_{t^{start}_{evcs}}^{t^{end}_{evcs}} t_{evcs} \ge T^{min}_{evcs} \quad (26)$$

In (III-A2)-(24), Equation (III-A2) and (13) represent the electrical power and heat balance of the microgrid. $\mu_{elec-boiler}$ is the efficiency of electric boiler. Equation (14) and (15) represent the capacity limitation of transformer between DN and MEG-E. S^{trans}_{elec} is the maximum power of transformer. Besides, BESS should satisfy the charge discharge rate and SOC constraints (16)-(18). $P^{max}_{bess,c}$ and $P^{max}_{bess,disc}$ are maximum permissible charging and discharging power. E^{MEG-E}_{bess} (t) is the amount of electricity stored in the battery at time t. SOC_{max} and SOC_{min} are maximum and minimum state of charge.

Equation (19) and (20) stand for the wind turbine operation constraints, and equation (21) and (22) stand for the PV operation constraints. P^{MEG-E}_{wind} (t) and P^{MEG-E}_{pv} (t) are wind power and photovoltaic output at time t. S^{max}_{wind} and S^{max}_{PV} are maximum rated power of wind power and photovoltaic. P^{max}_{wind} and P^{max}_{pv} are maximum power regulation rate of wind power and photovoltaic.

Equation (23) and (24) stand for the operation constraints of electric boiler. $S^{max}_{elec-boiler}$ is maximum rated power of electric boiler and $P^{max}_{elec-boiler}$ is maximum regulation rate of electric boiler. Electric vehicle can be charged slowly and quickly, which is limited by the maximum and minimum charging power limits. At the same time, in order to ensure the battery life, once the battery is charged, the whole charging process must be completed. The constraints can be expressed as (25) and (26). $P_{ev,max}$ and $P_{ev,min}$ are maximum and minimum charging power. T_{min} is the minimum charging time.

B. MATHEMATICAL MODEL OF MEG-S

1) OBJECTIVE FUNCTION

In order to meet different types of energy demand of users, MEG-S also operates gas network and its storage system. By purchasing the power of distribution network in low electricity price period, by using energy conversion and storage equipment, it can sell energy to users at high price when the energy demand is the highest and obtain the profits. Therefore, the objective function is described by (27).

$$\begin{aligned} min\ C_{MEG-S} = {} & C^{MEG-S}_{elec} + C^{MEG-S}_{anc} + C^{MEG-S}_{hydro} \\ & + C^{MEG-S}_{gt} + C^{MEG-S}_{caes} \\ & + C^{MEG-S}_{p2g} + C^{MEG-S}_{gas-boiler} - I^{MEG-S}_{user-elec} \\ & - I^{MEG-S}_{user-heat} - I^{MEG-S}_{user-gas} \end{aligned} \quad (27)$$

$$C^{MEG-S}_{gt} = \sum_{t=1}^{T} \frac{c_{gas}}{Q_{LHV}} \frac{P^{MEG-S}_{gt}(t)}{\eta_{gt}} \quad (28)$$

$$C^{MEG\text{-}S}_{hydro} = \sum_{t=1}^{T} \gamma_{hydro}\, P^{MEG\text{-}S}_{hydro}(t) \quad (29)$$

$$\begin{aligned} C^{MEG\text{-}S}_{caes} = {} & \sum_{t=1}^{T} \Big[\gamma_{caes\text{-}c}\, u^{MEG\text{-}S}_{caes\text{-}c}(t) P^{MEG\text{-}S}_{caes\text{-}c}(t) \\ & + \gamma_{caes\text{-}g}\, u^{MEG\text{-}S}_{caes\text{-}g}(t) P^{MEG\text{-}S}_{caes\text{-}g}(t) \Big] \end{aligned} \quad (30)$$

$$C^{MEG-S}_{p2\,g} = \sum_{t=1}^{T} \gamma_{p2\,g} P^{MEG-S}_{p2\,g}(t) \quad (31)$$

$$I^{MEG-S}_{user\text{-}gas} = \sum_{t=1}^{T} \tau^{MEG-S}_{user\text{-}gas}(t) \times Q^{MEG-S}_{user\text{-}gas}(t) \quad (32)$$

Different from MEG-E, MEG-S should have more schedulable power units to meet the power balance in order to make better use of the peak-valley energy price. It also has energy conversion equipment and large capacity energy storage equipment to meet the energy balance in order to make better use of the different price of multi-energy. Gas turbine and hydropower units are started at peak electricity price. The operating cost of gas turbine (C^{MEG-S}_{gt}) is shown in (28). C_{gas} is the price of gas. Q_{LHV} is the low calorific value of natural gas. $P^{MEG-S}_{gt}(t)$ is the output of micro gas turbine at time t and η_{gt} is the efficiency of gas turbine.

Hydropower units are connected by 10kV or lower voltage level, and are generally small capacity units of run-of-river type which will not affect the ecological flow and irrigation of rivers, so it is not necessary to consider the cost of abandoned water. The operation cost of hydropower units (C^{MEG-S}_{hydro}) mainly refers to the power consumption cost of hydropower station, as shown in (29). P^{MEG-S}_{hydro} is the output of hydropower unit at time t. γ_{hydro} is the generation cost factor of hydropower.

The air energy storage device in MEG-S adopts Advanced Adiabatic Compressed Air Energy Storage (AA-CAES) technology. AA-CAES system is composed of compressor, expander, gas storage chamber, heat accumulator, heat exchanger and other main components. AA-CAES can store the heat generated in the compression process in the heat accumulator, and use the heat stored in the process of power generation to reheat the air of the expander, which avoids the use of fossil fuel, improves the cycle efficiency, and also has the heating capacity. This article does not consider the investment and installation cost of AA-CAES system, but only considers the operation cost (C^{MEG-S}_{caes}), as shown

in (30). $P_{caes-c}^{MEG-S}(t)$ and $P_{caes-g}^{MEG-S}(t)$ are electric power under compressed air condition and power generation condition at time t. $u_{caes-c}^{MEG-S}(t)$ and $u_{caes-g}^{MEG-S}(t)$ are binary variable indicating that AA-CAES system is in compressed air or power generation condition. γ_{caes-c} and γ_{caes-g} are operating cost coefficient of compressed air condition and power generation condition.

The P2G device uses electric energy to produce gas through the synthesis reaction of electrolytic water and methane. P2G device can achieve the interconnection of power grid and natural gas network with gas turbine or fuel cell equipment. P2G is dispatched by MEG-S operators, so there is no separate power purchase cost. Therefore, the operation cost of P2G (C_{p2g}^{MEG-S}) only considers the maintenance cost, as shown in (31). $P_{p2g}^{MEG-S}(t)$ is the power consumed by P2G at time t. γ_{p2g} is the cost coefficient of operation and maintenance of P2G.

The revenue from selling gas to customers can be expressed in (32). $Q_{user-gas}^{MEG-S}(t)$ is gas consumption of users at time t and $\tau_{user-gas}^{MEG-S}(t)$ is the price of gas purchased by users at time t.

Besides, the operation of MEG-S also produces the cost of purchasing electricity from distribution network (C_{elec}^{MEG-S}), the cost of purchasing ancillary services from the distribution network(C_{anc}^{MEG-S}) and the revenue from electricity and heat sales to commercial users ($I_{user-elec}^{MEG-S}$, $I_{user-heat}^{MEG-S}$), which mathematical formulas can refer to (2)-(6) and (10)-(11).

2) MODEL CONSTRAINTS

The constraints of MEG-S can be given as below:

$$P_{elec}^{MEG-S}(t) + u_{case-c}^{MEG-S} P_{case-c}^{MEG-S}(t) + P_{p2g}^{MEG-S}(t) + P_{user-elec}^{MEG-S}(t) - P_{hydro}^{MEG-S}(t) - P_{gt}^{MEG-S}(t) - P_{pv}^{MEG-S}(t) - u_{case-g}^{MEG-S} P_{case-g}^{MEG-S}(t) = 0 \quad (33)$$

$$Q_{user-heat}^{MEG-S}(t) = \frac{1}{\mu_{gas-boiler}} P_{gas-boiler}^{MEG-S}(t) + \mu_{caes} P_{caes-c}^{MEG-S}(t) \quad (34)$$

$$G_{user-gas}^{MEG-S}(t) + G_{gas-boiler}^{MIEG-S}(t) + G_{gt}^{MEG-S}(t) - \eta_{p2g} P_{p2g}^{MEG-S}(t) - G_{gas-net}^{MEG-S}(t) = 0 \quad (35)$$

$$P_{gt,min}^{MEG-S} \le P_{gt}^{MEG-S}(t) \le P_{gt,max}^{MEG-S} \quad (36)$$

$$-P_{gt}^{max} \le P_{gt}^{MEG-S}(t+1) - P_{gt}^{MEG-S}(t) \le P_{gt}^{max} \quad (37)$$

$$P_{hydro,min}^{MEG-S} \le P_{hydro}^{MEG-S}(t) \le P_{hydro,max}^{MEG-S} \quad (38)$$

$$-P_{hydro}^{max} \le P_{hydro}^{MEG-S}(t+1) - P_{hydro}^{MEG-S}(t) \le P_{hydro}^{max} \quad (39)$$

$$P_{caes-c,min}^{MEG-S} \le P_{caes-c}^{MEG-S}(t) \le P_{caes-c,max}^{MEG-S} \quad (40)$$

$$-P_{caes-c}^{max} \le P_{caes-c}^{MEG-S}(t+1) - P_{caes-c}^{MEG-S}(t) \le P_{caes-c}^{max} \quad (41)$$

$$P_{caes-g,min}^{MEG-S} \le P_{caes-g}^{MEG-S}(t) \le P_{caes-g,max}^{MEG-S} \quad (42)$$

$$-P_{caes-g}^{max} \le P_{caes-g}^{MEG-S}(t+1) - P_{caes-g}^{MEG-S}(t) \le P_{caes-g}^{max} \quad (43)$$

$$u_{caes-c}^{MEG-S}(t) + u_{caes-g}^{MEG-S}(t) = 1 \quad (44)$$

$$E_{caes}^{air}(t) + \eta_{caes-air} P_{caes-air}^{MEG-S}(t) \le E_{caes}^{air-max} \quad (45)$$

$$E_{caes}^{heat}(t) + \eta_{caes-heat} P_{caes-heat}^{MEG-S}(t) \le E_{caes}^{heat-max} \quad (46)$$

$$G_{p2g}^{MEG-S}(t) = \eta_{p2g} P_{p2g}^{MEG-S}(t) \quad (47)$$

$$P_{p2g,min}^{MEG-S} \le P_{p2g}^{MEG-S}(t) \le P_{p2g,max}^{MEG-S} \quad (48)$$

$$-P_{p2g}^{max} \le P_{p2g}^{MEG-S}(t+1) - P_{p2g}^{MEG-S}(t) \le P_{p2g}^{max} \quad (49)$$

$$G_{gas-boiler}^{MEG-S}(t) = \frac{1}{\mu_{gas-boiler}} P_{gas-boiler}^{MEG-S}(t) \quad (50)$$

$$P_{gas-boiler,min}^{MEG-S} \le P_{gas-boiler}^{MEG-S}(t) \le P_{gas-boiler,max}^{MEG-S} \quad (51)$$

$$-P_{gas-boiler}^{max} \le P_{gas-boiler}^{MEG-S}(t+1) - P_{gas-boiler}^{MEG-S}(t) \le P_{gas-boiler}^{max} \quad (52)$$

In MEG-S, real time balance of electric energy, heat energy and natural gas are shown in (III-B2)-(III-B2). $\mu_{gas-boiler}$ and μ_{caes} are heat production efficiency of gas boiler and CAES. η_{p2g} is gas conversion efficiency of P2G. $G_{gas-net}^{MEG-S}(t)$, $G_{gas-boiler}^{MEG-S}(t)$ and $G_{gt}^{MEG-S}(t)$ are gas consumed from gas network and gas consumed of gas boiler and gas turbine.

Equation (36) and (37) represent output limit and climbing constraint of gas-turbine generator. $P_{gt,max}^{MEG-S}$ and $P_{gt,min}^{MEG-S}$ are upper and lower output limits of micro gas turbine. P_{gt}^{max} is the maximum power regulation rate of gas turbine. Equation (38) and (39) represent output limit and climbing constraint of hydropower generator. $P_{hydro,max}^{MEG-S}$ and $P_{hydro,min}^{MEG-S}$ are upper and lower output limits of hydropower. P_{hydro}^{max} is the maximum power regulation rate of hydropower.

During air compressed stage, AA-CAES consumes electricity and generates heat energy to heat storage tank. In power generation stage, compressed air expands and generates electricity. In this process, there is an electric power constraint, shown in (40)-(43). $P_{caes-c,max}^{MEG-S}$ and $P_{caes-c,min}^{MEG-S}$ are upper and lower power limits of air compressed stage. $P_{caes-g,max}^{MEG-S}$ and $P_{caes-g,min}^{MEG-S}$ are upper and lower power limits of power generation stage. P_{caes-c}^{max} and P_{caes-g}^{max} are the maximum power regulation rate of different states. At the same time, the CAES can only operate in either compressed air or power generation conditions, and the constraint is shown in (44). In addition, the energy storage constraint of AA-CAES are shown in (45)-(46) (the energy storage value has been converted into electric energy from volume). $E_{caes}^{air}(t)$ and $E_{caes}^{heat}(t)$ are energy storage value of compressed air storage device and heat tank at time t. And the maximum value of them can represented as $E_{caes}^{air-max}$ and $E_{caes}^{heat-max}$. $\eta_{caes-air}$ and $\eta_{caes-heat}$ are the power conversion efficiency in the compressed air and the heat storage tank.

Operation power limit and maximum regulation rate constraint of P2G and gas-boiler are shown in (47)-(52). $P_{p2g,max}^{MEG-S}$ and $P_{p2g,min}^{MEG-S}$ are maximum and minimum power of P2G. P_{p2g}^{max} is the maximum power regulation rate of P2G. $P_{gas-boiler,max}^{MEG-S}$ and $P_{gas-boiler,min}^{MEG-S}$ are upper and lower output limits of gas boiler.

Besides, the constraints of photovoltaic generation and transformer operation are the same as those in MEG-E, which can be referred to (14)-(15) and (21)-(22).

IV. REAL TIME ADAPTIVE DYNAMIC OPTIMIZATION STRATEGY BASED ON DEEP LEARNING

A. NONLINEAR OPTIMIZATION WITH MULTI-DIMENSIONAL CONSTRAINTS

According to the MEG mathematical model, we need to solve a multi-dimensional constrained nonlinear optimization problem. For constrained optimization, the general aim is to transform the problem into an easier subproblem that can be solved and used as the basis of an iterative process. The Karush-Kuhn-Tucker (KKT) equations are necessary conditions for optimality. If the problem is a convex optimizing problem, the KKT equations are both necessary and sufficient for a global solution point. The solution of the KKT equations forms the basis to many nonlinear programming algorithms. These algorithms attempt to compute the Lagrange multipliers directly. Constrained quasi-Newton methods guarantee super-linear convergence by accumulating second-order information regarding the KKT equations using a Quasi-Newton updating procedure. These methods are commonly referred to as Sequential Quadratic Programming (SQP) methods. At each major iteration, an approximation is made of the Hessian matrix of the Lagrange function using a Quasi-Newton updating method. And the matrix is used to generate a Quadratic Programming (QP) subproblem whose solution is used to form a search direction for a line search procedure [36]–[38]. The QP subproblem can be shown in (53).

$$\begin{aligned} &\min_{d\in R^n} \frac{1}{2}\mathbf{d}^{\mathrm{T}}\mathbf{H}_k\mathbf{d} + \nabla f(\mathbf{x}_k)^{\mathrm{T}}\mathbf{d} \\ &\nabla\ g_i(\mathbf{x}_k)d + g_i(\mathbf{x}_k)d = 0, i = 1, \ldots, m_e \\ &\nabla\ g_i(\mathbf{x}_k)d + g_i(\mathbf{x}_k)d \le 0, i = m_e + 1, \ldots, m \end{aligned} \tag{53}$$

And the method to updating the Hessian matrix can be shown in (54).

$$\begin{aligned} \mathbf{H}_{k+1} &= \mathbf{H}_k + \frac{\mathbf{q}_k\mathbf{q}_k^T}{\mathbf{q}_k^T\mathbf{s}_k} - \frac{\mathbf{H}_k\mathbf{s}_k\mathbf{s}_k^T\mathbf{H}_k^T}{\mathbf{s}_k^T\mathbf{H}_k\mathbf{s}_k} \\ where: \mathbf{s}_k &= \mathbf{x}_{k+1} - \mathbf{x}_k \\ \mathbf{q}_k &= \left(\nabla f(\mathbf{x}_{k+1}) + \sum_{i=1}^{m}\lambda_i{\cdot}\nabla g_i(\mathbf{x}_{k+1})\right) \\ &\quad - \left(\nabla f(\mathbf{x}_k) + \sum_{i=1}^{m}\lambda_i{\cdot}\nabla g_i(\mathbf{x}_k)\right) \end{aligned} \tag{54}$$

In addition, the improved particle swarm optimization algorithm and genetic algorithm can also be used to solve the optimal operation point of MEG. However, the above algorithms usually take a long time to calculate and can't deal with the power fluctuation and forecast deviation of generation side and demand side online. In the real time Adaptive Dynamic Optimization algorithm base on Deep Learning (ADO-DL) proposed in this article, the day ahead optimization of MEG operation is only the first step, so we can use the mature global optimization toolbox in MATLAB to solve the problem.

B. DEEP LEARNING OF MEG OPTIMAL OPERATION

Deep learning is a machine learning technology using deep neural network. Deep neural network is a multi-layer neural network with more than two hidden layers. The multi-layer neural network can be used to predict the input-output relationship of a complex nonlinear dynamic system through certain training. The MEG system proposed in this article is a dynamic nonlinear system with multiple energy sources. Although the traditional optimization algorithm can solve the problem, the traditional algorithm takes a relatively long time for calculation and can't meet the needs of real-time. This real-time output fluctuation is the inherent characteristics of small mountain distributed energy and small users.

If the deep neural network is trained directly by using massive historical operation data to make the network directly replace the input-output characteristics of MEG, a high-dimensional nonlinear system, there will be two problems: the storage and dynamic update of the massive historical optimal operation data, and the over fitting problem of training. Therefore, in this article, we consider only using the continuous recent historical optimal data to train the deep neural network, so that it can quickly get the initial point nearest to the optimal operation point in the subsequent online dynamic algorithm, so as to speed up the calculation convergence speed. In the pretraining process, we need to construct a multi-hidden layers deep neural network with multi input and output. Secondly, the historical operation data (obtained from the global optimization in advance) of the previous consecutive days are taken as the training data, and the training set and test set are divided, and the appropriate training algorithm is selected. Finally, the network training is implemented by using MATLAB deep learning toolbox. The pre-training process of action network using MEG optimal operation data is shown in Fig. 3.

C. REAL TIME ADAPTIVE DYNAMIC OPTIMIZATION STRATEGY

With the iterative Adaptive Dynamic Programming (ADP) algorithm of continuous system proposed by Murray *et al.* [39], the dynamic programming theory has made a great breakthrough. Then, the adaptive dynamic programming under constrained conditions is discussed. And the adaptive dynamic programming algorithms based on continuous time and discrete time are discussed, and proved the convergence of performance critic function in [40]-[41]. Furthermore, Cheng proved the convergence condition of neural network for implementing dynamic programming algorithm [42] and Liu proposed an improved Action Dependent Heuristic Dynamic Programming (ADHDP) [43].

ADP consists of three parts: dynamic system, action function and critic function. Each part can be replaced by neural network, in which the dynamic system can be modeled by neural network, the action network is used to approximate the optimal control strategy, and the critic network is used to approximate the optimal performance index function. After

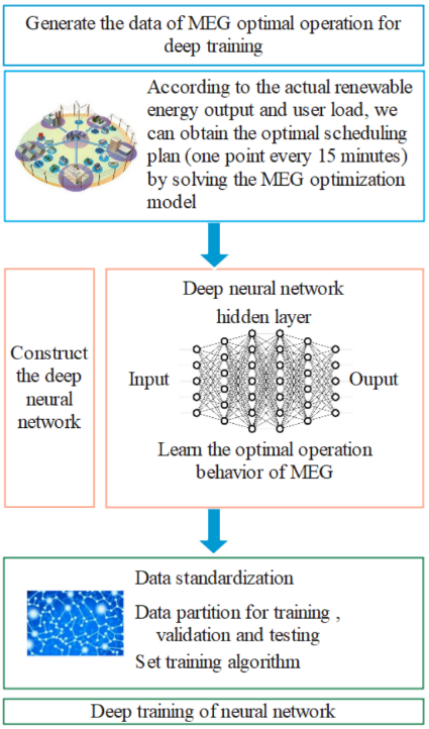

FIGURE 3. Pre-training process of action network using optimal operation date of MEG.

action acts on the dynamic system, the reward / penalty generated by the environment in different stages will affect the critic function. Then the function approximation structure or neural network is used to realize the approximation of action function and critic function. The parameter updating of critic function is based on the Bellman Optimal Principle, which can not only reduce the forward calculation time, but also respond to the dynamic changes of the unknown system online, so that it can automatically adjust some parameters in the network structure. However, ADHDP does not need model network, only contains action network and critic network. State variables and control variables are the input of critic network. Its structure is shown in Fig. 4.

The principle of ADHDP is to use the function approximate structure (neural network) to approach the performance indicator function and control strategy in the dynamic programming equation, so as to satisfy the principle of the highest priority, and obtain the optimal control and the optimal performance indicator function J, which can be expressed as (55).

$$J[\mathbf{x}(k), k] = \sum_{i=k}^{\infty} \gamma^{i-k} U[\mathbf{x}(k), \mathbf{u}(i), i] \tag{55}$$

where, U is utility function, γ is discounted factor. The output of critic network ($\hat{J}$), which is shown in (56), is the estimation of function J. $\mathbf{W}_c$ is the parameters of critic network.

$$\hat{J}(k) = \hat{J}\,[[\mathbf{x}(k), \mathbf{u}(k), k, \mathbf{W}_c]] \tag{56}$$

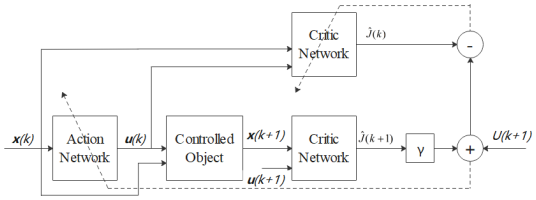

FIGURE 4. Structure of ADHDP.

By minimizing the error E_c, which is shown in (57), a trained critic network can be obtained.

$$\begin{aligned} \|E_c\| &= \sum_k E_c(k) \\ &= \frac{1}{2}\sum_k [\hat{J}(k) - U(k) - \gamma J(k+1)] \end{aligned} \tag{57}$$

The training of the action network is carried out by using the control signal $\mathbf{u}(k) = u[\mathbf{x}(k), k, \mathbf{W}_a]$ with the goal of minimizing $\hat{J}(k)$, which $\mathbf{W}_a$ is the parameters of action network. Once the action network is trained by minimizing the output of the critic network, a trained network will be obtained, which will produce the optimal or suboptimal control strategy.

For real time optimization of MEG operation, this article establishes a deep neural network as the critic network based on the ADHDP method, and uses the previously trained deep neural network to construct the action network and controlled object. Because the deep neural network has learned the optimal operation behavior of MEG, when the real-time distributed renewable energy output and user load are different from the predicted value, the deep neural network can immediately generate a system operation point which is close to the optimal operation point of the system, that is, the control strategy. At the same time, we can get an estimated value of performance indicator function after the control strategy is input into the critic network. Then, the performance indicator function J can converge rapidly by on-line iteration and training as shown in (55)-(57), and the optimal operation strategy of the system is obtained. The structure of proposed ADO-DL strategy is shown in Fig. 5.

In the optimization process of MEG, this article takes P_{wind}, P_{pv}, $P_{user-elec}$, $Q_{user-heat}$, $G_{user-gas}$, as state variables and P_{elec}, P_{evcs}, P_{bess}, P_{caes}, P_{hydro}, P_{gt}, $P_{gas-boiler}$, P_{p2g} as control variables into ADO-DL strategy, a flow chart of implementing ADO-DL strategy is shown in Fig. 6.

V. CASE STUDIES

A. SYSTEM DATA

In Guizhou power grid, distributed renewable energy and different types of users and equipment are integrated into the distribution network through 10kV transformers, and the limits of power exchange are defined as -1MW, 1MW. The energy demand data of users and the output data of renewable energy power plants are obtained from the actual participants actually connected to the power grid. To validate the effective-

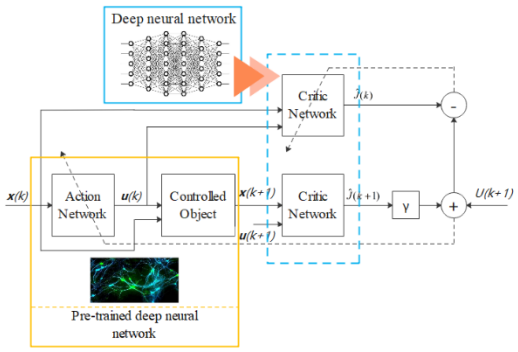

FIGURE 5. Structure of ADO-DL.

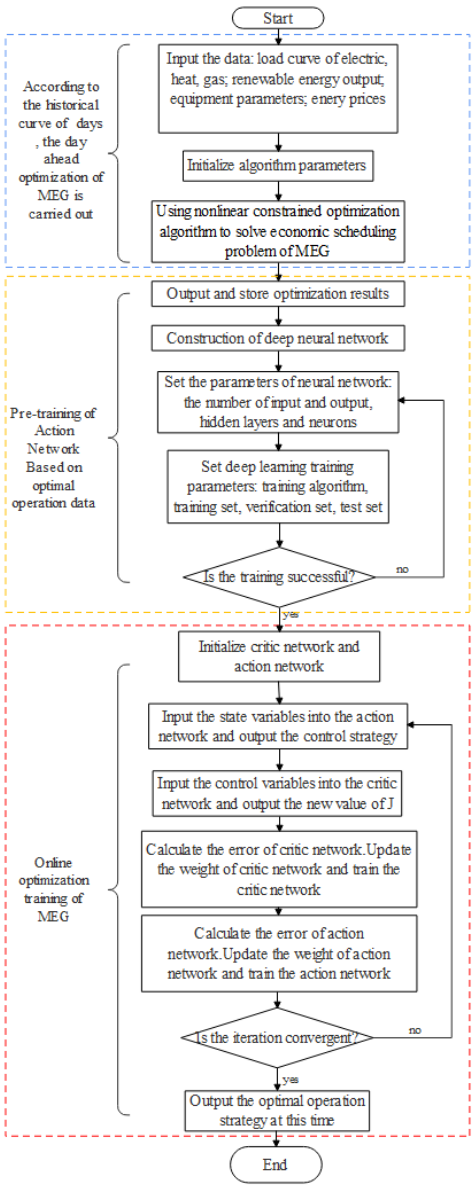

FIGURE 6. Procedures of proposed ADO-DL Strategy.

ness of the proposed models and method, two micro energy grids are studied, which constructed on the basis of operation characteristics of distributed wind power and photovoltaic power plants in northwest plateau mountainous areas of Guizhou and the actual microgrid. Besides, the simulations are implemented on a PC with Intel(R) Core (TM) i7 with two processors at 3.0GHZ.

TABLE 1. Parameters of equipment in MEG-E.

Wind Power	Capacity 1.5MW	S^{max}_{wind} 1.5MW	P^{max}_{wind} 0.5MW/min
PV	Capacity 1MW	S^{max}_{PV} 1MW	P^{max}_{pv} 0.4MW/min
BESS	$P^{max}_{bess,c}$ 0.3MW	$P^{max}_{bess,disc}$ 0.3MW	a_s 0.05
	SOC_{max} 1	SOC_{min} 0.2	β_s 0.6
EVCS	$P_{ev,max}$ 0.2MW	$P_{ev,min}$ 0.05MW	T_{min} 4hour
Electric-Boiler	$S^{max}_{elec\text{-}boiler}$ 0.2MW	$P^{max}_{elec\text{-}boiler}$ 0.17MW	$\mu_{elec\text{-}boiler}$ 0.9

B. COMPARATIVE STUDY BETWEEN MEG-E AND MEG-S

When different energy forms matching with a variety of energy conversion equipment and prosumer, MEG can have quite different operating characteristics. If the spatiotemporal characteristics of output and user load can be well matched, the system economy will be greatly improved and the solution space will be expanded. In order to verify that the coupling of multiple energy sources can make MEG operating more flexible and economic, it is necessary to compare the operation characteristics of MEG-E with relatively few energy types and MEG-S with more energy types and conversion equipment under the same scale system. At the same time, it is necessary to compare the operation characteristics of MEG-E and MEG-S with those under traditional power grid mode, so as to prove that MEG operation mode will bring higher security and economy.

This article constructs two systems of MEG-E and MEG-S, and makes the simulation according to the optimization model proposed in this article using 96 points data of one day. The parameters of equipment in MEG-E and MEG-S are shown in Table 1 and Table 2.

In this article, the data with 15 minutes timescale of wind power, photovoltaic, industrial users and commercial users in typical working days in winter are used for simulation. At the same time, the price of electricity purchased by MEG from the DN is set as 0.7 ¥/kWh, the price of auxiliary services purchased from the DN is 0.02 ¥/kW, the price of electricity sold to the DN is set as 0.6 ¥/kWh, the price of electricity sold to users is 0.7 ¥/kWh, and the price of heat sold to users (converted into electricity) is 1.5 ¥/kWh. It is assumed that the power of transformer from DN to MEG is in positive direction. When equipment in MEG charging, the power is positive. In order to show the operation ability of MEG-S as prosumer, the public gas network is connected with users but only providing emergency reserve. The capacity of P2G device is adequate to achieve the self-sufficient of gas in

TABLE 2. Parameters of equipment in MEG-S.

Hydropower	Capacity 0.3MW	γ_{hydro} 0.05	$P^{MEG\text{-}S}_{hydro,max}$ 0.2MW/min	$P^{MEG\text{-}S}_{hydro,min}$ 0.1MW/min
PV	Capacity 2MW	S^{max}_{PV} 1.8MW	P^{max}_{pv} 0.8MW/min	
CAES	Capacity 0.5MW	$P^{MEG\text{-}S}_{caes\text{-}c,max}$ 0.5MW/min	$\eta_{caes\text{-}heat}$ 0.3	$\eta_{caes\text{-}air}$ 0.2
	$P^{MEG\text{-}S}_{caes\text{-}c,min}$ 0.1MW/min	$P^{MEG\text{-}S}_{caes\text{-}g,max}$ 0.4MW/min	$P^{MEG\text{-}S}_{caes\text{-}g,min}$ 0.1MW/min	
Gas Turbine	P^{max}_{gt} 0.2MW	η_{gt} 0.35	$P^{MEG\text{-}S}_{gt,max}$ 0.2	$P^{MEG\text{-}S}_{gt,min}$ 0.1
P2G	P^{max}_{p2g} 0.8MW	$P^{MEG\text{-}S}_{p2g,max}$ 0.6MW/min	$P^{MEG\text{-}S}_{p2g,min}$ 0.4MW/min	η_{p2g} 0.81
Gas-Boiler	$P^{max}_{gas\text{-}boiler}$ 0.4MW	$P^{MEG\text{-}S}_{gas\text{-}boiler,max}$ 0.3MW/min	$P^{MEG\text{-}S}_{gas\text{-}boiler,min}$ 0.1MW/min	$\mu_{gas\text{-}boiler}$ 0.35

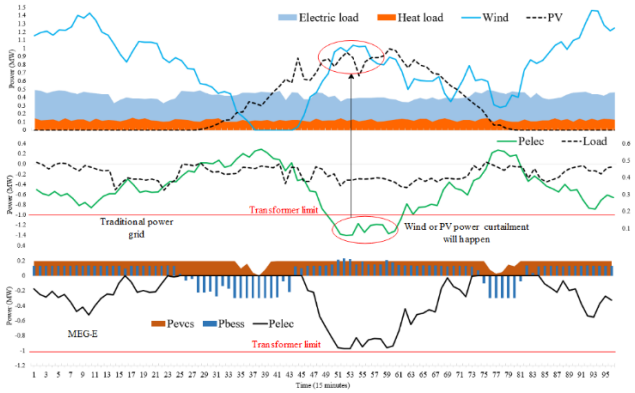

FIGURE 7. Optimization results of MEG-E.

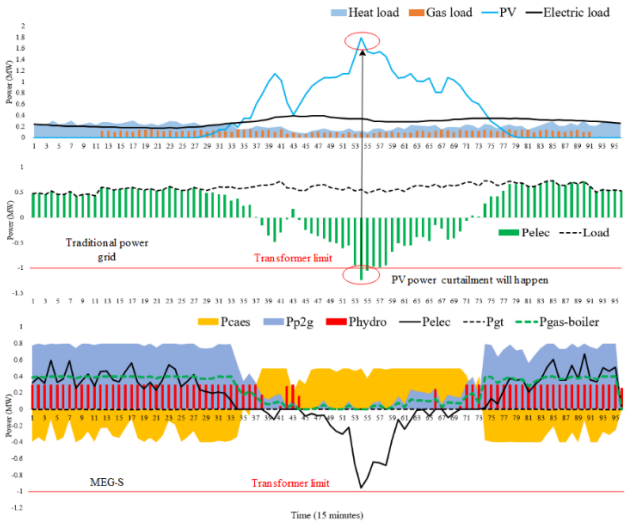

FIGURE 8. Optimization results of MEG-S.

MEG-S. The optimization results of MEG-E and MEG-S are shown in Fig. 7 and Fig. 8.

Through the optimization results of MEG-E, when the wind power and PV output reached the peak, it can be seen that under the same load level (in the traditional power grid operation mode, the thermal load of industrial users has been converted into electrical load), the transformer has a high probability of overload, leading to the difficulty of dispatching at traditional power grid mode without BESS, EVCS and other equipment. If active control is carried out, it will inevitably lead to wind or PV curtailment, which does not meet the policy of the government to fully absorb renewable energy. At the same time, it is also the practical dilemma faced by the power grid dispatching. If MEG-E mode is adopted, BESS and EVCS can be charged in the period when the renewable energy output is high, so as to ensure the safety of equipment and avoid static instability. At the same time, BESS can also release energy when the renewable energy output is low, reduce electricity purchased from DN, and improve system economy. In addition, according to the optimization results, it can be seen that in MEG-E, industrial users and a high proportion of wind power are coordinated, EVCS and BESS are jointly operated, which has better complementary characteristics. Through optimization, the daily minimum operating cost of MEG-E converges to ¥16604.

For the power grid integrated with PV, as the commercial users have demand for electric, heat and gas (for the traditional power grid, because there is no P2G, gas power generation and other equipment, the thermal load and gas load have been converted into electrical load), the distribution transformer may be overloaded in the period of load peak, resulting in the PV curtailment. MEG-S, which is connected with multi energy, has more flexible operation mode because of P2G, Gas- boiler, CAES and other energy coupling and storage equipment in the network. Through the conversion of different energy, MEG-S can operate economically, meet the demand of commercial users for different energy types, and greatly improve user satisfaction.

Comparing MEG-S with MEG-E, the two MEG operation modes are suitable for different users and energy forms. CAES and BESS play an important role in energy transfer and storage in both MEGs. MEG-S has the energy conversion equipment P2G, which makes the operation mode more flexible than MEG-E. At the same time, because there are more kinds of energy that can be sold to users, the operation economy of MEG-S is also better than MEG-E. In the simulation, one day operation of MEG-S can obtain a profit of ¥1549.

By optimizing the same scale MEG-E and MEG-S, we can get the conclusions. For the traditional power grid, due to the power equality constraint, when the renewable energy output is large and the load is small, the transformer will inevitably exceed the limit. At this time, in order to ensure the static stability of the power grid, wind or solar will be abandoned. Both MEG-E and MEG-S operation modes have enough adjustment measures to ensure system security and fully absorb renewable energy, which proves that MEG operation

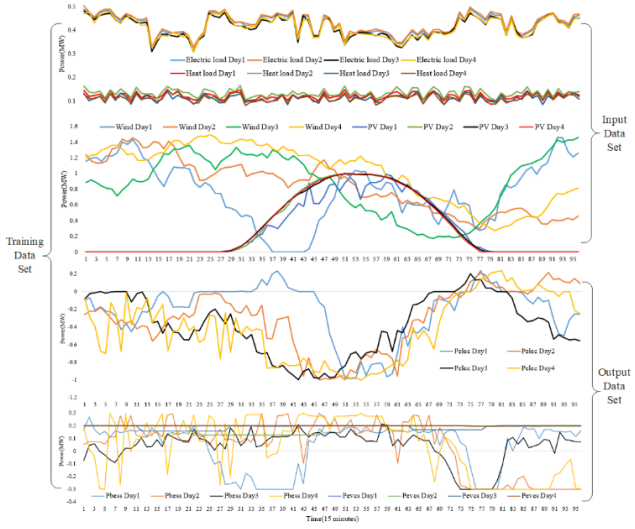

FIGURE 9. Training data set for deep learning of MEG optimal behavior.

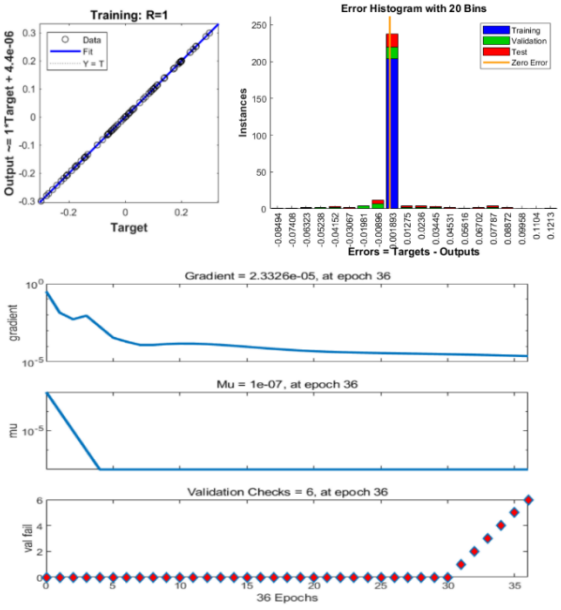

FIGURE 10. Deep training process of action network.

mode is better than traditional power grid mode. At the same time, compared with MEG-E, MEG-S has more energy forms and energy conversion equipment, and its operation flexibility is higher. It can guarantee operation constraints through energy conversion and space-time transfer, and obtain higher profit by using price difference. However, whether MEG-E or MEG-S is selected, it is necessary to assess the resource characteristics of renewable energy and the property of users in MEG, and the reasonable choice of operation mode can make MEG operating more economical.

C. VALIDATION OF PROPOSED ADO-DL STRATEGY

In order to learn the optimal operation behavior of MEG, we build a deep neural network with three hidden layers and 30 neurons in each layer in the MATLAB deep learning

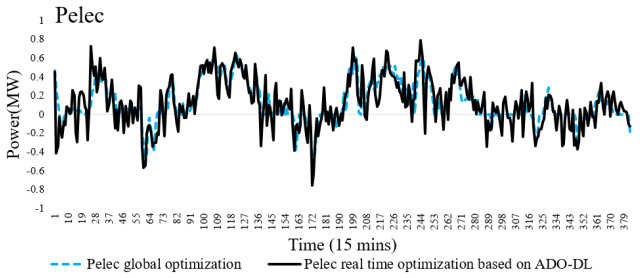

FIGURE 11. Optimization results comparison of transformer power.

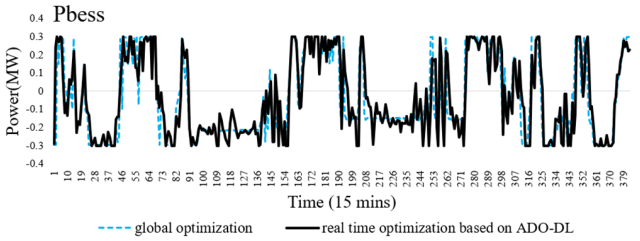

FIGURE 12. Optimization results comparison of BESS.

toolbox. The input layer of the neural network has 4 input variables and the output layer has 3 output variables. This article takes MEG-E as an example to achieve the training process of the deep neural network and verify the effectiveness of the ADO-DL strategy.

Firstly, the curves of PV, wind power, power load and heat load of users for 7 consecutive days are extracted from the real system, and the MEG model proposed in this article is used to solve the optimization problem, then we can obtain the optimal operation plan of MEG for each day. The data of the first four days are used for the pre-training of the action network (deep neural network). In the process of training, P_{wind}, P_{pv}, $P_{user-elec}$ and $Q_{user-heat}$, are taken as input variables, when P_{elec}, P_{evcs} and P_{bess}, are taken as output variables to form the training data set. The training data set is shown in Fig. 9. And Levenberg-Marquardt backpropagation algorithm is adopted for the training, the deep training result is shown in Fig. 10.

According to the training results, the action network has been trained well, and the deep neural network has learned the historical optimal operation behavior of MEG-E. Although the deep neural network at current training status can't fully explain the causal relationship between the input variables and output variables of MEG-E model, the pre-trained action network can provide an initial iteration point which is close to the optimal operation point for the subsequent online adaptive dynamic optimization and improve the computational efficiency.

After training the action network and initializing the critical network, the online optimization stage is in progress. In order to verify the correctness and reliability of the online optimization algorithm, the input data of the last three days of 8 days are input into MEG-E optimization model for global optimization, and the optimization results are used as the standard data to judge whether the calculation results of

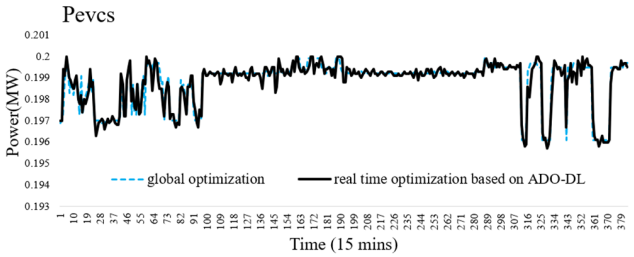

FIGURE 13. Optimization results comparison of EVCS.

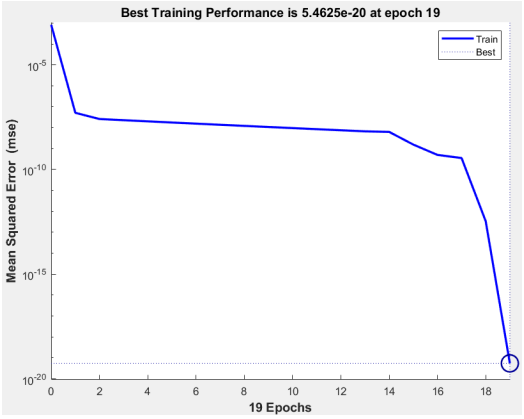

FIGURE 14. Training epochs and error.

online optimization algorithm are correct. If the data of the next four days are input one by one online, and the optimizing result of decision variables is the same as that of global optimization, we can confirm that the online optimization algorithm is reliable. After online optimization simulation of three consecutive days, the online optimization results of MEG-E are compared with the global optimization results calculated before. The results are shown in Fig. 11- Fig. 13.

Through the comparison of the optimization results, the online optimization operation plan of each time obtained by using ADO-DL is almost consistent with the global optimal operation plan. At the same time, when the ADO-DL algorithm is used to optimize and train 384 consecutive running points for 4 days on line, the longest convergence time is 9.219328s, the shortest is 0.242512s, and the mean squared error reaches the minimum value of 5.4625×10^{-20} at the 19th epoch, as shown in Fig. 14. Therefore, the effectiveness and real-time performance of ADO-DL strategy can be verified by the above optimization results. Meanwhile, the slightly different operation points between ADO-DL and global optimization results are also feasible suboptimal solutions under system constraints, which can also meet the needs of system operation security.

The power output of distributed wind power and photovoltaic units in plateau mountainous areas is greatly affected by local climate and has strong uncertainty. Considering the investment cost, MEG operators has no willingness to invest in complex and expensive wind and PV power prediction system for distributed and small capacity installed units. Although the energy users will not change energy consumption habit in a short time, they have different energy supply forms and the change of different energy price will lead to the converting demand between different energy forms. Therefore, the research of online optimization algorithm with real-time control performance is the key to solve the uncertainty in MEG operation. The process of online optimization in this article, the wind power, photovoltaic and user load data in the last four days are input into the ADO-DL algorithm as a series of unknown data. The action network and critical network in ADO-DL are not trained by these data. Therefore, it is verified that the ADO-DL algorithm proposed in this article can deal with the uncertainty of MEG operation online.

Distributed renewable energy and industrial or commercial users together constitute MEG. This kind of prosumer consumes energy to create value while producing energy. While seeking maximum profit, MEG operators also bear social responsibility and government pressure, that is, they must fully absorb renewable energy. The ADO-DL strategy proposed in this article can achieve this goal well, and improve the operation efficiency of multi energy coupling system.

VI. CONCLUSION

According to the characteristics of energy production and consumption of different prosumer, this article constructs the optimization model of MEG-E and MEG-S, then carries out optimization simulation and comparative study. Furthermore, in order to fully absorb renewable energy and solve the uncertainty of distributed energy output, a real-time dynamic optimization strategy of MEG based on deep learning (ADO-DL) is proposed, the correctness and performance of the algorithm are verified by consecutive days online optimization. Some conclusions can be drawn from the study of this article.

1) The reasonable matching of different distributed renewable energy, different users and equipment can improve the operation economy of MEG. That is, by matching energy storage equipment and energy conversion equipment reasonably, the feasible operating range of MEG can be expanded and the optimal operation point can be found more quickly.

2) In ADO-DL, the pretraining of action network can make the iteration of online optimization approach the optimal operation point quickly, so as to improve the real time performance of the algorithm.

3) The operation problem of MEG is an optimization problem of high-dimensional nonlinear systems with time-delay. The relationship between input variables and optimal output can be quickly found by learning massive historical operation data through deep learning technology.

In this article, the model of internal operation process of energy conversion equipment in MEG is simplified. At the same time, the flexibility of MEG operation will be improved if the user's real-time load response and real-time price are considered in the follow-up study.

REFERENCES

[1] J. Hu, Y. Li, and H. Zhou, "Energy management strategy for a society of prosumers under the IoT environment considering the network constraints," *IEEE Access*, vol. 7, pp. 57760–57768, 2019.

[2] Z. Zhao, J. Guo, X. Luo, J. Xue, C. S. Lai, Z. Xu, and L. L. Lai, "Energy transaction for multi-microgrids and internal microgrid based on blockchain," *IEEE Access*, vol. 8, pp. 144362–144372, 2020, doi: 10.1109/ACCESS.2020.3014520.

[3] D. Xu, Q. Wu, B. Zhou, C. Li, L. Bai, and S. Huang, "Distributed multi-energy operation of coupled electricity, heating, and natural gas networks," *IEEE Trans. Sustain. Energy*, vol. 11, no. 4, pp. 2457–2469, Oct. 2020.

[4] S. Xie, Z. Hu, J. Wang, and Y. Chen, "The optimal planning of smart multi-energy systems incorporating transportation, natural gas and active distribution networks," *Appl. Energy*, vol. 269, pp. 1–20, Jul. 2020.

[5] S. Lauria, F. Palone, M. Schembari, and M. Maccioni, "Very long distance connection of gigawatt-size offshore wind farms: Extra high-voltage AC versus high-voltage DC cost comparison," *IET Renew. Power Gener.*, vol. 10, no. 5, pp. 713–720, May 2016.

[6] Y. Wang, "Very long distance connection of gigawatt-size offshore wind farms extra high-voltage AC versus high-voltage DC cost comparison," *IET Gener. Transmiss. Distrib.*, vol. 11, pp. 330–338, Oct. 2016.

[7] F. Scheller and T. Bruckner, "Energy system optimization at the municipal level: An analysis of modeling approaches and challenges," *Renew. Sustain. Energy Rev.*, vol. 105, pp. 444–461, May 2019.

[8] Z. Li and Y. Xu, "Temporally-coordinated optimal operation of a multi-energy microgrid under diverse uncertainties," *Appl. Energy*, vol. 240, pp. 719–729, Feb. 2019.

[9] J. Wei, Y. Zhang, J. Wang, X. Cao, and M. A. Khan, "Multi-period planning of multi-energy microgrid with multi-type uncertainties using chance constrained information gap decision method," *Appl. Energy*, vol. 260, pp. 1–19, Dec. 2019.

[10] N. Liu, L. Zhou, C. Wang, X. Yu, and X. Ma, "Heat-electricity coupled peak load shifting for multi-energy industrial parks: A Stackelberg game approach," *IEEE Trans. Sustain. Energy*, vol. 11, no. 3, pp. 1858–1869, Jul. 2020.

[11] C. Li, H. Yang, M. Shahidehpour, Z. Xu, B. Zhou, Y. Cao, and L. Zeng, "Optimal planning of islanded integrated energy system with solar-biogas energy supply," *IEEE Trans. Sustain. Energy*, vol. 11, no. 4, pp. 2437–2448, Oct. 2020.

[12] B. Zhou, D. Xu, C. Li, C. Y. Chung, Y. Cao, K. W. Chan, and Q. Wu, "Optimal scheduling of biogas-solar-wind renewable portfolio for multicarrier energy supplies," *IEEE Trans. Power Syst.*, vol. 33, no. 6, pp. 2437–2448, Nov. 2018.

[13] M. Xie, X. Ji, X. Hu, P. Cheng, Y. Du, and M. Liu, "Autonomous optimized economic dispatch of active distribution system with multi-microgrids," *Energy*, vol. 153, pp. 479–489, Jun. 2018.

[14] H. Ali, A. Hussain, V.-H. Bui, and H.-M. Kim, "Consensus algorithm-based distributed operation of microgrids during grid-connected and islanded modes," *IEEE Access*, vol. 8, pp. 78151–78165, 2020.

[15] Y. Du, Z. Wang, G. Liu, X. Chen, H. Yuan, Y. Wei, and F. Li, "A cooperative game approach for coordinating multi-microgrid operation within distribution systems," *Appl. Energy*, vol. 222, pp. 383–395, Jul. 2018.

[16] H. Xu, Z. Meng, R. Zhao, Y. Wang, and Q. Yan, "Optimal dispatching strategy of an electric-thermal-gas coupling microgrid considering consumer satisfaction," *IEEE Access*, vol. 8, pp. 173169–173176, 2020, doi: 10.1109/ACCESS.2020.3024931.

[17] J. H. Zheng, C. Q. Wu, J. Huang, Y. Liu, and Q. H. Wu, "Multi-objective optimization for coordinated day-ahead scheduling problem of integrated electricity-natural gas system with microgrid," *IEEE Access*, vol. 8, pp. 86788–86796, 2020.

[18] Z. Tang, S. Lin, W. Liang, Y. Xie, Y. Song, J. Wang, and M. Liu, "Optimal dispatch of integrated energy campus microgrids considering the time-delay of pipelines," *IEEE Access*, vol. 8, pp. 178782–178795, 2020, doi: 10.1109/ACCESS.2020.3026344.

[19] D. Xu, B. Zhou, K. W. Chan, C. Li, Q. Wu, B. Chen, and S. Xia, "Distributed multienergy coordination of multimicrogrids with biogas-solar-wind renewables," *IEEE Trans. Ind. Informat.*, vol. 15, no. 6, pp. 3254–3266, Jun. 2019.

[20] A. Wang and W. Liu, "Distributed incremental cost consensus-based optimization algorithms for economic dispatch in a microgrid," *IEEE Access*, vol. 8, pp. 12933–12941, 2020.

[21] T. Liu, X. Tan, B. Sun, Y. Wu, and D. H. K. Tsang, "Energy management of cooperative microgrids: A distributed optimization approach," *Int. J. Electr. Power Energy Syst.*, vol. 96, pp. 335–346, Mar. 2018.

[22] Y. He, W. Wang, and X. Wu, "Multi-agent based fully distributed economic dispatch in microgrid using exact diffusion strategy," *IEEE Access*, vol. 8, pp. 7020–7030, 2019.

[23] H. Gu, Y. Li, J. Yu, C. Wu, T. Song, and J. Xu, "Bi-level optimal low-carbon economic dispatch for an industrial park with consideration of multi-energy price incentives," *Appl. Energy*, vol. 262, pp. 1–20, Jan. 2020.

[24] R. Rigo-Mariani, S. O. C. Wae, S. Mazzoni, and A. Romagnoli, "Comparison of optimization frameworks for the design of a multi-energy microgrid," *Appl. Energy*, vol. 257, pp. 1–13, Oct. 2019.

[25] H. Gao, S. Xu, Y. Liu, L. Wang, Y. Xiang, and J. Liu, "Decentralized optimal operation model for cooperative microgrids considering renewable energy uncertainties," *Appl. Energy*, vol. 262, pp. 1–11, Jan. 2020.

[26] R. Aboli, M. Ramezani, and H. Falaghi, "Joint optimization of day-ahead and uncertain near real-time operation of microgrids," *Int. J. Electr. Power Energy Syst.*, vol. 107, pp. 34–46, May 2019.

[27] L. Yao, X. Wang, T. Ding, Y. Wang, X. Wu, and J. Liu, "Stochastic day-ahead scheduling of integrated energy distribution network with identifying redundant gas network constraints," *IEEE Trans. Smart Grid*, vol. 10, no. 4, pp. 4309–4322, Jul. 2019.

[28] M. Sedighizadeh, G. Shaghaghi-Shahr, M. Esmaili, and M. R. Aghamohammadi, "Optimal distribution feeder reconfiguration and generation scheduling for microgrid day-ahead operation in the presence of electric vehicles considering uncertainties," *J. Energy Storage*, vol. 21, pp. 58–71, Feb. 2019.

[29] S. Leonori, M. Paschero, F. M. F. Mascioli, and A. Rizzi, "Optimization strategies for microgrid energy management systems by genetic algorithms," *Appl. Soft Comput.*, vol. 86, pp. 1–13, Jan. 2020.

[30] W. M. Ferreira, I. R. Meneghini, D. I. Brandao, and F. G. Guimarães, "Preference cone based multi-objective evolutionary algorithm applied to optimal management of distributed energy resources in microgrids," *Appl. Energy*, vol. 274, pp. 1–15, Jun. 2020.

[31] H. Xiao, W. Pei, W. Deng, L. Kong, H. Sun, and C. Tang, "A comparative study of deep neural network and meta-model techniques in behavior learning of microgrids," *IEEE Access*, vol. 8, pp. 30104–30118, 2020.

[32] J. Reynolds, M. W. Ahmad, Y. Rezgui, and J.-L. Hippolyte, "Operational supply and demand optimisation of a multi-vector district energy system using artificial neural networks and a genetic algorithm," *Appl. Energy*, vol. 235, pp. 699–713, Feb. 2019.

[33] H. Nie, Y. Chen, Y. Xia, S. Huang, and B. Liu, "Optimizing the post-disaster control of islanded microgrid: A multi-agent deep reinforcement learning approach," *IEEE Access*, vol. 8, pp. 153455–153469, 2020, doi: 10.1109/ACCESS.2020.3018142.

[34] O. Samuel, N. Javaid, A. Khalid, W. Z. Khan, M. Y. Aalsalem, M. K. Afzal, and B.-S. Kim, "Towards real-time energy management of multi-microgrid using a deep convolution neural network and cooperative game approach," *IEEE Access*, vol. 8, pp. 161377–161395, 2020, doi: 10.1109/ACCESS.2020.3021613.

[35] J. Reynolds, M. W. Ahmad, Y. Rezgui, and J.-L. Hippolyte, "Operational supply and demand optimization of a multi-vector district energy system using artificial neural networks and a genetic algorithm," *Appl. Energy*, vol. 259, pp. 1–21, Nov. 2019.

[36] M. Powell, "The convergence of variable metric methods for nonlinearly constrained optimization calculations," in *Nonlinear Programming 3*. New York, NY, USA: Academic, 1978.

[37] M. Powell, "A fast algorithm for nonlinearly constrained optimization calculations," *Numer. Anal.*, vol. 630, pp. 485–500, Nov. 1978.

[38] M. J. D. Powell, "Variable metric methods for constrained optimization," in *Computing Methods in Applied Sciences and Engineering* (Lecture Notes in Mathematics), vol. 704, R. Glowinski, J. L. Lions, and I. Laboria, Eds. Berlin, Germany: Springer, 1979, doi: 10.1007/BFb0063615.

[39] J. J. Murray, C. J. Cox, G. G. Lendaris, and R. Saeks, "Adaptive dynamic programming," *IEEE Trans. Syst. Man, Cybern. B, Cybern.*, vol. 32, no. 2, pp. 140–153, Oct. 2002.

[40] T. Hanselmann, L. Noakes, and A. Zaknich, "Continuous-time adaptive critics," *IEEE Trans. Neural Netw.*, vol. 18, no. 3, pp. 631–647, May 2007.

[41] A. Al-Tamimi, F. L. Lewis, and M. Abu-Khalaf, "Discrete-time nonlinear HJB solution using approximate dynamic programming: Convergence proof," *IEEE Trans. Syst. Man, Cybern. B, Cybern.*, vol. 38, no. 4, pp. 943–949, Aug. 2008.

[42] T. Cheng, F. L. Lewis, and M. Abu-Khalaf, "A neural network solution for fixed-final time optimal control of nonlinear systems," *Automatica*, vol. 43, no. 3, pp. 482–490, Mar. 2007.
[43] D. Liu and H. Zhang, "A neural dynamic programming approach for learning control of failure avoidance problems," *Int. J. Intell. Control Syst.*, vol. 10, pp. 21–32, Oct. 2005.

SU AN (Graduate Student Member, IEEE) received the B.S. degree in electrical engineering and automation from Southwest Jiaotong University, Sichuan, China, in 2010, and the M.S. degree in automation of electric power system from North China Electric Power University, Beijing, China, in 2013. He is currently pursuing the Ph.D. degree in management science and engineering with Guizhou University, Guiyang, Guizhou, China.

From 2013 to 2020, he has worked as the Chief Dispatcher of the Power Dispatching Control Center, Guizhou Power Grid Company. At the same time, he is also the third-level Assistant Technical Expert of Guizhou Power Grid. He has rich experience in the operation of large ac/dc power grids and economic dispatch of power grid. His main research interests include optimal operation of distributed renewable energy in Plateau and mountainous areas, the optimal operation of micro energy grid combined with artificial intelligence technology, the extraction of operation characteristics of large power grid under the energy Internet systems, and joint operation optimization of multi-microgrid in active distribution networks.

HONGLEI WANG received the Ph.D. degree in management science and engineering from the Chinese Academy of Sciences, China, in 2007. He is currently a Professor with the School of Management and the School of Electrical Engineering, Guizhou University (GZU), China; the Director of the Key Laboratory of "Internet+" Collaborative Intelligent Manufacturing in Guizhou Province; the Executive Director of the China Society of systems engineering; the Director of the China Society of optimal selection, overall planning and economic mathematics; the Chairman of the Guizhou System Engineering Society; and the Vice President of the Guizhou Automation Society. In the past three years, 11 papers have been published in major journals and international conferences. His current research interests include manufacturing big data and intelligent manufacturing, and management system engineering (optimization and decision making). His research was funded by the National Natural Science Foundation of China. He has won the Second and Third prizes of Science and Technology Progress in Guizhou Province.

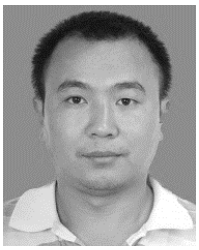

XUFENG YUAN received the Ph.D. degree in power system and its automation from the Huazhong University of Science and Technology, China, in 2007. He is currently a Professor with the School of Electrical Engineering, Guizhou University (GZU), China. His current research interests include power electronic of distribution networks and optimal operation of micro grid.